LETTERS

Massively parallel manipulation of single cells and microparticles using optical images

Pei Yu Chiou[1], Aaron T. Ohta[1] & Ming C. Wu[1]

The ability to manipulate biological cells and micrometre-scale particles plays an important role in many biological and colloidal science applications. However, conventional manipulation techniques—including optical tweezers[1–6], electrokinetic forces (electrophoresis[7,8], dielectrophoresis[9], travelling-wave dielectrophoresis[10,11]), magnetic tweezers[12,13], acoustic traps[14] and hydrodynamic flows[15–17]—cannot achieve high resolution and high throughput at the same time. Optical tweezers offer high resolution for trapping single particles, but have a limited manipulation area owing to tight focusing requirements; on the other hand, electrokinetic forces and other mechanisms provide high throughput, but lack the flexibility or the spatial resolution necessary for controlling individual cells. Here we present an optical image-driven dielectrophoresis technique that permits high-resolution patterning of electric fields on a photoconductive surface for manipulating single particles. It requires 100,000 times less optical intensity than optical tweezers. Using an incoherent light source (a light-emitting diode or a halogen lamp) and a digital micromirror spatial light modulator, we have demonstrated parallel manipulation of 15,000 particle traps on a 1.3 × 1.0 mm^2 area. With direct optical imaging control, multiple manipulation functions are combined to achieve complex, multi-step manipulation protocols.

Light-patterned electrodes have been widely used in xerography, which was invented in 1942[18]. This concept was recently applied to patterning of colloidal structures[19,20]; optically-induced electrophoresis was used to attract charged particles onto indium tin oxide (ITO)[19]and semiconductor[20] surfaces. However, none of the previous literature has shown the capability of single-particle manipulation. Our optoelectronic tweezers (OET) utilize direct optical images to create high-resolution dielectrophoresis (DEP) electrodes for the parallel manipulation of single particles. DEP force results from the interaction of the induced dipoles in particles subjected to a non-uniform electric field[9]. The magnitude of the force depends on the electric field gradient and the polarizability of the particle, which is dependent on the dielectric properties of the particle and the surrounding medium. DEP is a well established technique, and has been widely used to manipulate micrometre and submicrometre particles as well as biological cells[21,22]. Travelling-wave DEP is particularly attractive for high-throughput cell manipulation without external liquid pumping[10,11]. The travelling electric field produced by a multi-phase alternating current (a.c.) bias on a parallel array of electrodes levitates and transports many particles simultaneously. However, travelling-wave DEP cannot resolve individual particles. Recently, a programmable DEP manipulator with an individually addressable two-dimensional electrode array has been realized using complementary metal-oxide-semiconductor (CMOS) integrated circuit technology[23]: parallel manipulation of a large number (~10,000) of cells was demonstrated. The CMOS DEP manipulator has two potential drawbacks: first, the need of on-chip integrated circuits increases the cost of the chip, making it less attractive for disposable applications; and second, the trap density (~400 sites mm^{-2}) is also limited by the size of the control circuits.

Figure 1 illustrates the OET device structure used in our experiments. The liquid containing the cells or particles of interest is sandwiched between a upper transparent, conductive ITO-coated glass, and a lower photoconductive surface, which consists of multiple featureless layers of ITO-coated glass, an n+ hydrogenated amorphous silicon (a-Si:H) layer, an undoped a-Si:H layer, and a silicon nitride layer. These two surfaces are biased with an a.c. signal,

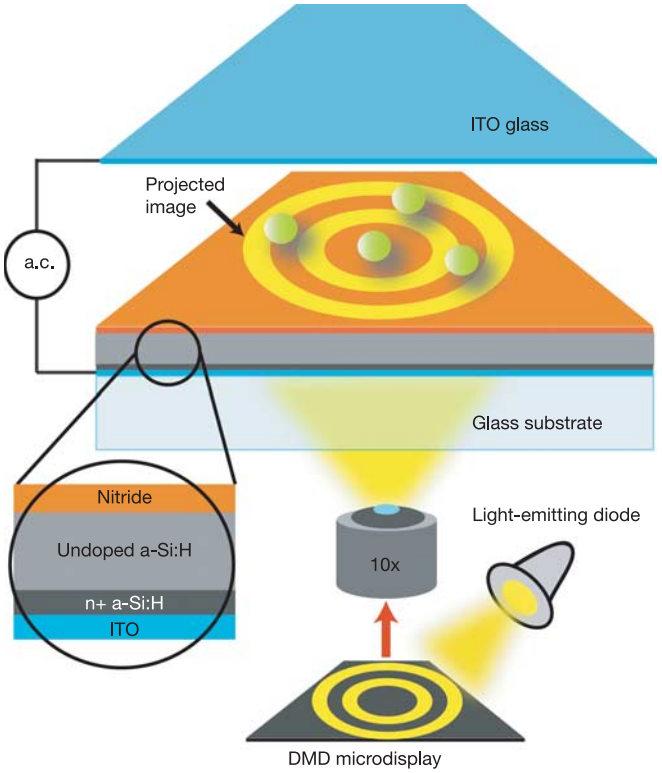

Figure 1 | Device structure used in optoelectronic tweezers. Liquid that contains microscopic particles is sandwiched between the top indium tin oxide (ITO) glass and the bottom photosensitive surface consisting of ITO-coated glass topped with multiple featureless layers: 50 nm of heavily doped hydrogenated amorphous silicon (a-Si:H), 1 μm of undoped a-Si:H, and 20 nm of silicon nitride. The top and bottom surfaces are biased with an a.c. electric signal. The illumination source is an light-emitting diode operating at a wavelength of 625 nm (Lumileds, Luxeon Star/O). The optical images shown on the digital micromirror display (DMD) are focused onto the photosensitive surface and create the non-uniform electric field for DEP manipulation.

[1]Department of Electrical Engineering and Computer Sciences, and Berkeley Sensor and Actuator Centre (BSAC), University of California at Berkeley, California 94720, USA.

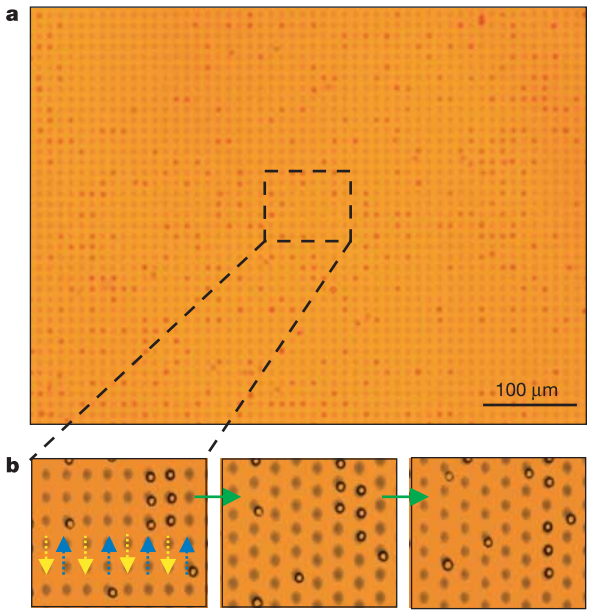

Figure 2 | Massively parallel manipulation of single particles. **a**, 15,000 particle traps are created across a 1.3 mm × 1.0 mm area. The 4.5-μm-diameter polystyrene beads experiencing negative DEP forces are trapped in the darker circular areas. Each trap has a diameter of 4.5 μm, which is adjusted to fit a single particle. **b**, Parallel transportation of single particles. Three snapshots from the video show the particle motion in part of the manipulation area. The trapped particles in two adjacent columns move in opposite directions, as indicated by the blue and yellow arrows.

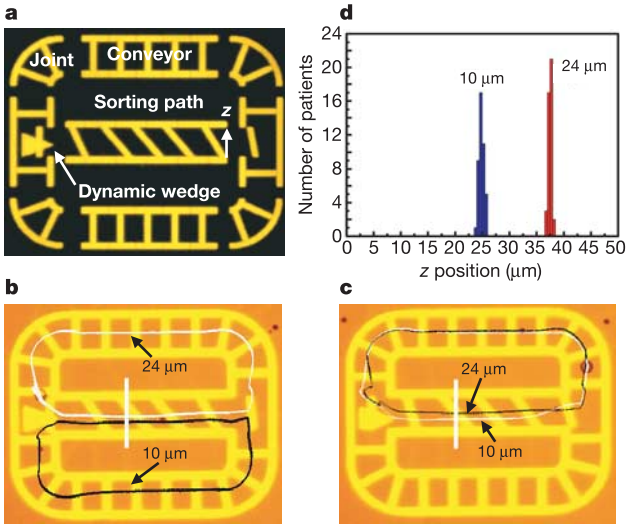

Figure 3 | An example of an integrated virtual optical machine. **a**, Integration of virtual components, including an optical sorter path, conveyors, joints and a wedge. The motion of different components is synchronized. **b**, **c**, Two polystyrene particles with sizes of 10 μm and 24 μm pass through the sorter path and are fractionated in the *z* direction owing to the asymmetrical optical patterns. The particle trajectories can be switched at the end of the sorter path by the optical wedge. **d**, Optical sorting repeatability test. The white and black loops in **b** and **c** represent the particle traces after 43 cycles. The trace broadening at the white bar has a standard deviation of 0.5 μm for the 10-μm bead and 0.15 μm for the 24-μm bead.

10 V peak-to-peak. When projected light illuminates the photoconductive layer, it turns on the virtual electrodes, creating non-uniform electric fields and enabling particle manipulation via DEP forces. These featureless layers are made without photolithography in fabrication, making the device inexpensive and attractive for disposable applications. The OET-based optical manipulation has two operational modes, positive OET and negative OET, as a result of the DEP forces induced for actuation. Particles can be attracted by or repelled from the illuminated area, depending on the a.c. electric field frequency and the particle's internal and surface dielectric properties.

Thanks to the photoconductive gain, the minimum optical intensity required to turn on a virtual electrode is 10 nW μm^{-2}, which is 100,000 times lower than that used in optical tweezers. This opens up the possibility of using incoherent optical images to control the DEP forces over a large area. The optical images are created by combining a light-emitting diode and a digital micromirror spatial light modulator (Texas Instruments, 1,024 × 768 pixels, 13.68 μm × 13.68 μm pixel size). The pattern is imaged onto the photoconductive surface through a 10 × objective. The resulting pixel size of the virtual electrode is 1.52 μm. The illumination source is a red light-emitting diode (625 nm wavelength) with a 1-mW output power (measured after the objective lens), which is sufficient to actuate 40,000 pixels. Tight focusing is not required for OET, and the optical manipulation area can be magnified by choosing an appropriate objective lens. Using a 10 × objective, the manipulation area (1.3 mm × 1.0 mm) is 500 times larger than that of optical tweezers.

Patterning high-resolution virtual electrodes is critical for achieving single-particle manipulation. OET has higher resolution than the optically-induced electrophoretic methods reported previously[19,20]. The minimum size of the virtual electrode is limited by the lateral diffusion length of the photogenerated carriers in the photoconductor, as well as the optical diffraction of the objective lens. The large number of electronic defect states in undoped a-Si:H results in a short ambipolar electron diffusion length of less than 115 nm (ref. 24). The ultimate virtual electrode resolution is thus determined by the optical diffraction limit. In addition, the induced OET force is proportional to the gradient of the square of the electric field, making it well confined to the local area of the virtual electrodes, which is also a key property for single-particle manipulation. A demonstration of the high-resolution capabilities of OET is the creation of 15,000 DEP traps across an area of 1.3 × 1.0 mm^2 (Fig. 2). The particles are trapped in the darker circular areas by the induced negative DEP forces, which push the beads into the non-illuminated regions, where the electric field is weaker. The size of each trap is optimized to capture a single 4.5-μm-diameter polystyrene bead. By programming the projected images, these trapped particles can be individually moved in parallel (Fig. 2b, and Supplementary Movie 1). Compared with the programmable CMOS DEP chip[23], the particle trap density

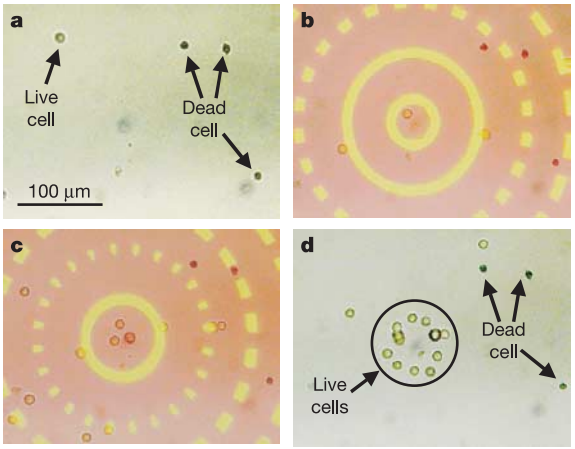

Figure 4 | Selective collection of live cells from a mixture of live and dead cells. **a**, Randomly positioned cells before OET. **b**, **c**, Cell sorting. The live cells experience positive OET, trapping them in the bright areas, and pulling the live cells into the pattern's centre. The dead cells (stained with Trypan blue dye) leak out through the dark gaps and are not collected. The optical pattern has a yellowish colour, while weak background scattered light results in a pinkish hue in the non-patterned areas. **d**, Sorted cells.

of OET (11,500 sites mm^{-2}) is 30 times higher, thanks to the high-resolution addressing ability.

Although OET has the capability to pattern high-resolution virtual electrodes, the trapping of submicrometre particles requires a strong electric field gradient to overcome brownian motion. In our current OET, the electric field gradient patterned by the light-emitting diode is not strong enough to trap particles less than 1 μm through the DEP mechanism. However, the trapping of particles 1 μm or less in diameter does occur when we operate our present device at a low-frequency a.c. bias (~1 kHz). (See Supplementary Movie 2.) This trapping mechanism is not due to DEP forces, but is caused by optically-patterned electrokinetic flow. Details of this mechanism are still under investigation.

Using direct imaging, sophisticated virtual electrodes can be easily patterned and reconfigured to create dynamic electric field distributions for continuous particle manipulation without the assistance of fluidic flow. Figure 3 shows an example of an integrated optical manipulator that combines the functions of optical conveyors, sorters, wedges and joints. Particles are transported through different functional areas and recycled in this light-patterned circuit, travelling through different paths depending on the position of the wedge divider. Particles with different sizes are fractionated in the lateral z direction as they pass through the sorter path, owing to the asymmetric shape of the light-patterned electric fields. At the end of the sorter path, an optical wedge divides and guides the particles into the two conveyors. The looped optical conveyors recycle the particles back to the sorter input to repeat the process (see Supplementary Movie 3). Figure 3b, c shows that the paths of the fractionated particles can be switched by reconfiguring the tip position of the optical wedge. The trajectories of the particle movement are highly repeatable and accurately defined. Figure 3d shows distribution of the particle position in the middle of the sorter (marked by a white bar) after the particles have passed through the sorter 43 times. The standard deviations of trace broadening are 0.5 μm for the 10-μm bead, and 0.15 μm for the 24-μm bead. As the magnitude of the DEP force is proportional to the particle volume, the larger particle shows a better confinement in the optically-patterned DEP cages during transportation.

By exploiting the dielectric differences between different particles or cells, DEP techniques have been able to discriminate and sort biological cells that have differences in membrane properties (permeability, capacitance and conductivity), internal conductivity, and size[21,25,26]. The OET technique not only inherits these DEP advantages, but also provides the capability of addressing each individual cell. We demonstrate the selective concentration of live human B cells from a mixture of live and dead cells in Fig. 4. The cells are suspended in an isotonic buffer medium of 8.5% sucrose and 0.3% dextrose, mixed with a solution of 0.4% Trypan blue dye to check the cell viability, resulting in a conductivity of 10 mS m^{-1}. The applied a.c. signal is 14 V peak-to-peak at a frequency of 120 kHz. The cell membranes of live cells are selectively permeable, and can maintain an ion concentration differential between the intracellular and extracellular environments. Dead cells cannot maintain this differential. When dead cells are suspended in a medium with a low ion concentration, the ions inside the cell membrane are diluted through ion diffusion. This results in a difference between the dielectric properties of live and dead cells[21]. Live cells experience positive OET, and are collected in the centre of the shrinking optical ring pattern by attraction to the illuminated region, while dead cells experience negative OET and are not collected (see Supplementary Movie 4).

Single-cell analysis is an important technique in comprehending many biological mechanisms, as it looks at the spectrum of response of each individual cell under stimulation. In addition to biological applications, the high-resolution electric field patterned on the OET surface could also serve as a dynamic template to guide the crystallization of colloidal structures.

Received 27 March; accepted 11 May 2005.

1. Grier, D. G. A revolution in optical manipulation. *Nature* **424,** 810–816 (2003).
2. Ashkin, A., Dziedzic, J. M. & Yamane, T. Optical trapping and manipulation of single cells using infrared-laser beams. *Nature* **330,** 769–771 (1987).
3. MacDonald, M. P., Spalding, G. C. & Dholakia, K. Microfluidic sorting in an optical lattice. *Nature* **426,** 421–424 (2003).
4. Curtis, J. E., Koss, B. A. & Grier, D. G. Dynamic holographic optical tweezers. *Opt. Commun.* **207,** 169–175 (2002).
5. McGloin, D., Spalding, G. C., Melville, H., Sibbett, W. & Dholakia, K. Three-dimensional arrays of optical bottle beams. *Opt. Commun.* **225,** 215–222 (2003).
6. Garces-Chavez, V., Dholakia, K. & Spalding, G. C. Extended-area optically induced organization of microparticles on a surface. *Appl. Phys. Lett.* **86,** 031106 (2005).
7. Kremser, L., Blaas, D. & Kenndler, E. Capillary electrophoresis of biological particles: Viruses, bacteria, and eukaryotic cells. *Electrophoresis* **25,** 2282–2291 (2004).
8. Cabrera, C. R. & Yager, P. Continuous concentration of bacteria in a microfluidic flow cell using electrokinetic techniques. *Electrophoresis* **22,** 355–362 (2001).
9. Hughes, M. P. Strategies for dielectrophoretic separation in laboratory-on-a-chip systems. *Electrophoresis* **23,** 2569–2582 (2002).
10. Pethig, R., Talary, M. S. & Lee, R. S. Enhancing traveling-wave dielectrophoresis with signal superposition. *IEEE Eng. Med. Biol. Mag.* **22,** 43–50 (2003).
11. Morgan, H., Green, N. G., Hughes, M. P., Monaghan, W. & Tan, T. C. Large-area travelling-wave dielectrophoresis particle separator. *J. Micromech. Microeng.* **7,** 65–70 (1997).
12. Yan, J., Skoko, D. & Marko, J. F. Near-field-magnetic-tweezer manipulation of single DNA molecules. *Phys. Rev. E* **70,** 011905 (2004).
13. Lee, H., Purdon, A. M. & Westervelt, R. M. Manipulation of biological cells using a microelectromagnet matrix. *Appl. Phys. Lett.* **85,** 1063–1065 (2004).
14. Hertz, H. M. Standing-wave acoustic trap for nonintrusive positioning of microparticles. *J. Appl. Phys.* **78,** 4845–4849 (1995).
15. Kessler, J. O. Hydrodynamic focusing of motile algal cells. *Nature* **313,** 218–220 (1985).
16. Sundararajan, N., Pio, M. S., Lee, L. P. & Berlin, A. A. Three-dimensional hydrodynamic focusing in polydimethylsiloxane (PDMS) microchannels. *J. Microelectromech. Syst.* **13,** 559–567 (2004).
17. Lee, G. B., Hwei, B. H. & Huang, G. R. Micromachined pre-focused M x N flow switches for continuous multi-sample injection. *J. Micromech. Microeng.* **11,** 654–661 (2001).
18. Pai, D. M. & Springett, B. E. Physics of electrophotography. *Rev. Mod. Phys.* **65,** 163–211 (1993).
19. Hayward, R. C., Saville, D. A. & Aksay, I. A. Electrophoretic assembly of colloidal crystals with optically tunable micropatterns. *Nature* **404,** 56–59 (2000).
20. Ozkan, M., Bhatia, S. & Esener, S. C. Optical addressing of polymer beads in microdevices. *Sens. Mater.* **14,** 189–197 (2002).
21. Gascoyne, P. *et al.* Microsample preparation by dielectrophoresis: isolation of malaria. *Lab Chip* **2,** 70–75 (2002).
22. Krupke, R., Hennrich, F., von Lohneysen, H. & Kappes, M. M. Separation of metallic from semiconducting single-walled carbon nanotubes. *Science* **301,** 344–347 (2003).
23. Manaresi, N. *et al.* A CMOS chip for individual cell manipulation and detection. *IEEE J. Solid-State Circuits* **38,** 2297–2305 (2003).
24. Schwarz, R., Wang, F. & Reissner, M. Fermi-level dependence of the ambipolar diffusion length in amorphous-silicon thin-film transistors. *Appl. Phys. Lett.* **63,** 1083–1085 (1993).
25. Becker, F. F. *et al.* Separation of human breast-cancer cells from blood by differential dielectric affinity. *Proc. Natl Acad. Sci. USA* **92,** 860–864 (1995).
26. Yang, J., Huang, Y., Wang, X. B., Becker, F. F. & Gascoyne, P. R. C. Differential analysis of human leukocytes by dielectrophoretic field-flow-fractionation. *Biophys. J.* **78,** 2680–2689 (2000).

Supplementary Information is linked to the online version of the paper at www.nature.com/nature.

Acknowledgements We thank E.R.B. McCabe, U. Bhardwaj, R. Sun and F. Yu at UCLA for providing cultured human B cells for our experiments. We also thank A. Wheeler for technical advice regarding our cell experiments. This project is supported by the Center for Cell Mimetic Space Exploration (CMISE), a NASA University Research, Engineering and Technology Institute (URETI), and the Defense Advanced Research Project Agency (DARPA). P.Y.C acknowledges support from the Graduate Research and Education in Adaptive Bio-Technology (GREAT) training program. A.T.O acknowledges support from a National Science Foundation fellowship.

Author Information Reprints and permissions information is available at npg.nature.com/reprintsandpermissions. The authors declare no competing financial interests. Correspondence and requests for materials should be addressed to M.C.W. (wu@eecs.berkeley.edu).